https://www.doi.org/10.53964/jmge.2022005

https://www.innovationforever.com

Journal of Modern Green Energy

ISSN 2790-3206 (Online)

Open Access

Research Article

Modeling and Validation of PV Solar-Thermoelectric Generators Using Magnetized Nanofluids

Samuel Sami Howard[1,2]

[1]TransPacific Energy, Inc, Carson City, NV, USA

[2]IES, University of North Dakota, Grand Forks, ND, USA

[*]**Correspondence to: Samuel Sami Howard**, PhD, Professor, TransPacific Energy, Inc, 204 West Spear Street, Carson City, NV 89183, USA; Email: dr.ssami@transpacenergy.com

Received: December 9, 2021 **Accepted:** February 17, 2022 **Published:** September 5, 2022

Abstract

Objective: To develop a simulation model to predict the behavior of a hybrid system composed of a PV-Thermal panel and thermoelectric generator (TEG) using magnetized nanofluids.

Methods: The model has been established after the energy and mass conservation equations for magnetized nanofluids coupled with the heat transfer equations nanofluids for Al_2O_3, CuO, Fe_3O_4, and SiO_2, and the key parameters of the TEG.

Results: The concentrations of the nanoparticles vary from 1% up to 50%. flow under different magnetic field forces up to 17500 Gauss to study the dynamic behavior of the PV-Thermal panels, and integrated TEGs. The model has been validated using different experiments under different.

Conclusion: The model has fairly been compared with existing data, nanofluid particle concentrations and different solar radiation conditions.

Keywords: PV-Thermal panels, TEG, nanofluids, dynamic thermal behavior, numerical model, simulation, experimental data, and validation

Citation: Howard SS. Modeling and Validation of PV Solar-Thermoelectric Generators Using Magnetized Nanofluids. *J Mod Green Energy*, 2022; 1: 5. DOI: 10.53964/jmge.2022005.

1 INTRODUCTION

Thermoelectric generators (TEG) are "devices that convert temperature differences into electricity and thermal heat. TEGs are composed of several thermoelectric modules which are solid-state integrated circuits. These devices are established after the well-established thermoelectric well-known effects; the Peltier, Seebeck, and Thomson effects and have been presented and discussed[1-31]. TEGs are driven by heat sources as an energy drivers such as gas or oil flame, stove, campfire, industrial machinery, furnace, electricity, and solar energy. PV solar panels convert solar radiations into usable electricity and can generate

maximum rated power depending upon the intensity of solar radiation."

Recently, Yildiz et al.[10] compared solar panels with TEGs. Their study dealt with "different parameters such as efficiency, power generation capability and capacity, cost, size, potential consumer applications, and system installation complexity to generate power. It has been reported by Yildiz et al.[10], that two separate laboratory environments were created to measure the power outputs and efficiencies. Both devices were tested at different locations due to different operating environmental conditions. A solar PV module was tested under sunlight whereas a TEG module was tested inside an air conditioner condenser unit on the same test. The test results compared the two energy generating systems and discussed potential applications"

Furthermore, Dziurdzia and Tan[12] studied and showed the viability of "modeling complex phenomena occurring in thermoelectric devices and coupled simulations of both thermal and electrical processes utilizing electronic circuits simulators. Dziurdzia and Tan[12] built-in procedures for solving differential and nonlinear equations, the electronic circuit SPICE-like simulators that can be used for simulation of other electrical phenomena. SPICE provided a reliable electrothermal model for the Peltier module. The energy conversion and distribution flow can be simulated in an autonomous sensor node."

More recently, Sami and Marin[20] developed and presented "a numerical model studying the impact of nanofluids. the TEG has been studied and analyzed under different nanofluid particle concentrations and different solar radiation conditions. The nanofluids Al_2O_3, CuO, Fe_3O_4, and SiO_2 circulate in PV-Thermal solar panels and drive the TEG. In addition, numerical results also showed that the nanofluid Fe_3O_4 has the highest thermal heat transfer to HTF and the highest TEG and hybrid efficiencies. The model fairly compared with existing data".

Recently, a model for "geometry optimization of thermoelectric devices in a hybrid photovoltaic-thermoelectric system was presented by Freunek et al[23]. The model was intended to determine the optimal geometry of thermoelectric modules at which the maximum power output is achieved. The simulated results showed that an increase in both the overall power output and conversion efficiency can be achieved by incorporating a TEG for waste heat recovery from the photovoltaic (PV) cell and also demonstrated that the geometry optimization needs to consider the "trade-off" between achieving a large power output and minimizing the consumption of thermoelectric materials. During the study, Sagadevan[32] presented, a model to analyze the characteristics of the nanofluids fluid flow and compared the model's prediction to data published in the literature. He showed an increase in the efficiency of the PV-Th systems."

Significant research has been reported in the literature "on the improvement of the efficiency of PVs', Some studies[24-38] developed and implemented "novel concepts of combined photovoltaic-thermal solar panels and different heat transfer fluids (HTF), nanofluid. Knowing the thermal properties of nanofluids is essential to understanding their thermal behavior. More recently, Sagadevan[32] and Sani et al.[38] presented a study, on the thermal characteristic's nanoparticles Al_2O_3, CuO, Fe_3O_4, and SiO_2 circulating underneath a PV panel and thermal tank, in addition, Sagadevan[32] defined nanofluid as suspensions of nano-sized particles.

Sami[39] developed a "functional fluid consisting of a stable colloidal suspension of maghemite magnetic nanoparticles in water that was characterized from the points of view of thermoelectrical and optical properties, to evaluate its potential for direct electricity generation from the thermoelectric effect enabled by the absorption of sunlight. Their findings demonstrated that nanofluids have high promise as a HTF for co-generating heat and power in brand new hybrid flat-plate solar thermal collectors where top-heating geometry is imposed".

In this paper, a "mathematical model is presented hereby to describe the heat and mass balances of the nanofluids flow that absorbs the excess heat released from the PV-Th solar panels and drives the TEG modules. The model has been established after the energy and mass conservation equations coupled with the heat transfer equations of the nanofluids. The results are discussed and compared with experimental data published in the open literature to validate the model under different operating conditions such as solar radiations, nanofluid flow rates, ambient temperatures, and various volumetric nanofluid concentrations."

2 MATERIALS AND METHODS

2.1 Mathematical Model

The PV-Th solar hybrid system driving an integrated TEG is shown in Figure 1. The system is composed of a PV-Th collector, TEG, thermal tank for domestic hot water use. and monitoring system. The thermal tank was equipped with a heat exchanger to supply the heat for domestic or industrial use. The PV-Thermal loop has a thin parallel tubes heat exchanger welded on the backside and has direct contact with the PV solar panel for cooling down the PV solar cells. The flow in each tube has been divided into different elements (control volumes) to permit the finite-difference formulation and analysis of the flow. It is assumed in this model that; the nanofluid is homogeneous, isotropic, incompressible, Newtonian, and inlet velocity and inlet temperature are constant, and also thermophysical properties of the nanofluids are constant. In the following, the conservation mass and energy equations are written and

presented for nanofluids.

2.2 Solar PV Model

The solar PV panel is constructed of various modules and each module consists of arrays and cells. The dynamic current output can be obtained from the published articles[24-31,33] in terms of output single-phase current of the PV module, Light generated current per module, reverse saturation current per module, Terminal voltage per module, and Boltzmann constant among other parameters. The PV cell temperature, Tc, is influenced by various factors such as solar radiations, ambient conditions, and wind speed. It is well known that the cell temperature impacts the PV output current, and performance and its time-variation can be determined from the published articles[24-34]. The AC power of the inverter output P(t) is calculated using the inverter efficiency η_{inv}, output voltage between phases, neutral V_{fn}, for single-phase current, I_o and the power factor, $cos\varphi$ as follows:

$$P(t) = \sqrt{3}\eta_{inv} V_{fn} I_o cos\varphi \qquad (1)$$

2.3 PV Thermal Model

It is assumed in this model that all PV cells behave the same; therefore, this model can be applied to the whole PV solar panel. This model is an extension of the work presented by Sami and Campoverde[26]. The thermal heat absorbed by the PV solar cell can be calculated by the following equations[24-31,33];

$$Q_{in} = \alpha_{abs} G S_p \qquad (2)$$

Where,
α_{abs}: Overall absorption coefficient,
G: Total Solar radiation incident on the PV module,
S_p: Total area of the PV module.

Meanwhile, the PV cell temperature is computed from the following heat balance[31,37];

$$mC_{p\_module} \frac{dT_C}{dt} = Q_{in} - Q_{conv} - Q_{elect} \qquad (3)$$

Where,
T_C: PV cell temperature,
mC_{p_module}: Thermal capacity of the PV module,
t: time,
Q_{in}: Energy received due to solar irradiation, equation (2),
Q_{conv}: Energy loss due to convection,
Q_{elect}: Electrical power generated.

Interested readers in the detailed calculations of the terms; Q_{in}, Q_{conv}, and Q_{elect} in equation (3) are advised to consult references from Liang et al.[25,26,31,32].

2.4 Thermal Energy Incident in a PV Cell

The thermal energy transferred from the PV cells to the HTF is determined by the heat balance across the PV cell and HTF in terms of the heat transfer mechanisms; conduction, convection, and radiation as follows[25,26,31]; In addition, the heat transport fluid temperature is obtained after;

$$Q_{convection} = h_{water} \times \Delta T(T_m - T_f) \qquad (4)$$

$Q_{convection}$: Energy due to convection
h_{water}: Heat transfer coefficient
T_f: Fluid temperature

Each HTF tube is divided into several finite control volumes, and where thermophysical and thermodynamic properties are assumed constant at each element;

$$T_f = T_{f\_in} + \frac{\partial Q}{m_{water} C_p} \times t \qquad (5)$$

$\dot{m}_w$: Water mass flow (HTF)
C_p: Specific heat of the water
t: Time
∂Q: The heat transfer per element
T_{f_in}: Fluid temperature at the inlet.

The thermal energy transferred from the back of the PV cell to the HTF is obtained by

$$Q_{Thermal} = \dot{m} \times C_{p\_water} \times \Delta T(T_{fHx+1} - T_{f\_In}) \qquad (6)$$

Where,
$Q_{Thermal}$: Energy from the thermal process,
T_{fHx+1}: Fluid temperature at thermal element (f+1),
$T_{f\text{-}In}$: Fluid temperature at thermal element (1).

The total energy transferred to HTF is calculated from the integration of equations (5) and (6) written for each element, dx, along the length of each tube. Interested readers in the integration process can consult references[24,25,31].

2.5 Nanofluid HTF

The thermophysical, thermodynamic, and heat transfer properties of nanofluids are determined in terms of the volumetric concentration of the nanoparticles;

$$\alpha_{total} = \alpha_{particles} + \alpha_{base\ fluid} \qquad (7)$$

Where α represents the thermophysical property of the nanofluid.

The nanofluid thermal and thermophysical properties, α_{total}, can be calculated as follows:

$$\alpha_{total} = \alpha_{base\ fluid} + \alpha_{particles}(\Phi) \qquad (8)$$

Where, Φ represents the nanoparticles' volumetric

https://www.doi.org/10.53964/jmge.2022005

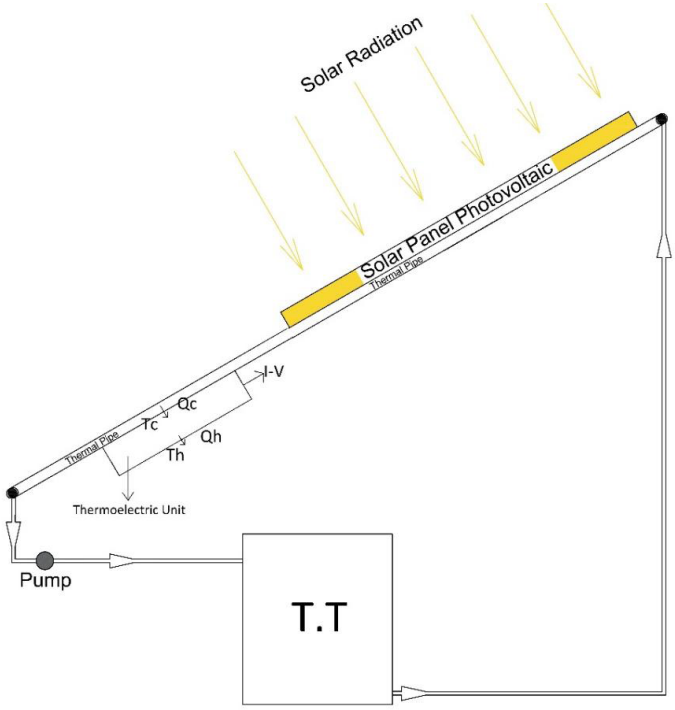

Figure 1. Integrated thermoelectric PV/Thermal hybrid system with Nanofluids[20].

concentration.

The thermal conductivity to thermal diffusivity and density of the nanofluids are related as[32,40]:

$$\lambda = \alpha \, \delta \, C_p \qquad (9)$$

Where C_p is the specific heat, α is the thermal diffusivity, and λ and ρ represent the thermal conductivity and density, respectively.

Equations (8) through (10) can be used to determine other thermophysical properties such as; α is the thermal diffusivity, λ and ρ represent the thermal conductivity and density as different magnetic forces Gauss published in the literature properties[9,10,20] as a function of the properties outlined in the Table 1.

2.5 Thermoelectric Model

As shown in Figure 2 when a temperature differential is maintained across the thermoelectric device, the voltage is generated and called the Seebeck emf, which is proportional to the magnitude of the temperature difference.

The heat balance across the thermoelectric unit shown in Figure 2 can be given by;

$$Q_c = Q_h + P_{out} \qquad (10)$$

Where Q_c is thermal heat defined by equation (10). Q_h and P_{out} represent the heat released to ambient and power output generated by the thermoelectric unit, respectively[13,20].

The thermal energy released Q_h from the thermoelectric unit can be obtained by MATLAB iteration using the following equation and the energy balance in the equation (10), Patel et al.[13] and Sami and Marin[20];

$$Q_h=(S_M \times Tc \times I)-(0.5 \times I^2 \times R_M)-(K_M \times DT) \qquad (11)$$

S_M is the Seebeck coefficient of the module in volts/°K, and T is the average module temperature in °K.

$$S_M = (S_{MTh} - S_{MTc}) / \Delta T \qquad (12)$$

Where: S_{MTh} is the module's Seebeck coefficient at the hot side temperature Th, S_{MTc} is the module's Seebeck coefficient at the cold side temperature Tc, R_M is the module's resistance in ohms and ΔT is the average module temperature in °K

Where,

$$\Delta T = Th - Tc$$

The output voltage (V_{out}) to the module in volts is obtained from Patel et al.[13] and Sami and Marin[20].

$$V_{out}t=(S_M \times \Delta T) + (I \times R_M) \qquad (13)$$

The electrical output power (P_{out}) to the module in watts is:

$$P_{out}=V_{out} \times I \qquad (14)$$

Where,

I: the output current to the module expressed in amperes,

V_{out}: the output voltage to the module expressed in volts,

Th: the hot side temperature of the module expressed in °K,

Tc: the cold side temperature of the module expressed

https://www.doi.org/10.53964/jmge.2022005

Table 1. Thermophysical Properties of Magnetized Nanofluids

	Al_2O_3	CuO	Fe_3O_4	SiO_2
C_{pnf}	b=0.1042a+6226.5	b=0.2011a+5730.8	b=0.8318a+4269.8	b=0.6187a+4293.2
K_{nf}	b=2E-05a+1.4888	b=5E-05a+1.3703	b=0.0002a+1.0209	b=0.0001a+1.0265
h	b=0.0031a+73.092	b=0.0031a+73.073	b=0.003a+73.225	b=0.003a+73.231

Where "b" represents the nanofluid-specific property and "a" is the magnetic field force in Gauss. C_{pnf}, K_{nf}, and h are the specific heat, thermal conductivity, and heat transfer coefficients of nanofluids.

in °K.

The efficiency of the solar PV panels can be expressed as follows:

$$\eta_{pv} = \frac{Q_{elec}}{Q_{colector}} \qquad (15)$$

Where, Q_{elec} is calculated by equation (2) and, $Q_{colector}$ is obtained by equation (3).

The thermal efficiency of thermal energy transferred to the HTF is:

$$\eta_{Qth} = \frac{Q_{th}}{Q_{colector}} \qquad (16)$$

Where Q_{th} is calculated by equation (2).

Finally, the hybrid system energy conversion efficiency for harnessing energy from solar energy using integrated thermoelectric photovoltaic-thermal solar panels and nanofluids can be determined using terms calculated in equations (1) and (7) to be formulated as:

$$\eta_{sh} = \frac{Q_{th} + Q_{elec}}{Q_{colector}} \qquad (17)$$

Where, Q_{elec} is calculated by equation (1) Q_{th} is calculated by equation (7).

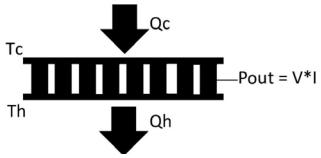

Figure 2. Thermoelectric cell[20].

2.6 Numerical Procedure

Equations (1) through (17) describe the "energy conversion process in the PV-Th panels, TEG unit concept with nanofluids that have been shown in the flow diagram in Figure 2, The numerical computations outlined in Figure 3, start with the input of the parameters of the PV-Thermal solar panel, thermal tubes, TEG device, nanoparticles; Al_2O_3, CuO, Fe_3O_4, and SiO_2, solar radiations, and magnetic fields. The equations were integrated into the finite-difference formulations. Iterations were performed using MATLAB iteration techniques until a converged solution is reached. Then the thermophysical properties and the heat transfer characteristics of the base fluid, water, and nanofluids at different concentrations are determined by solving the finite-difference formulation of the aforementioned equations. Finally, the individual and hybrid system efficiencies were calculated".

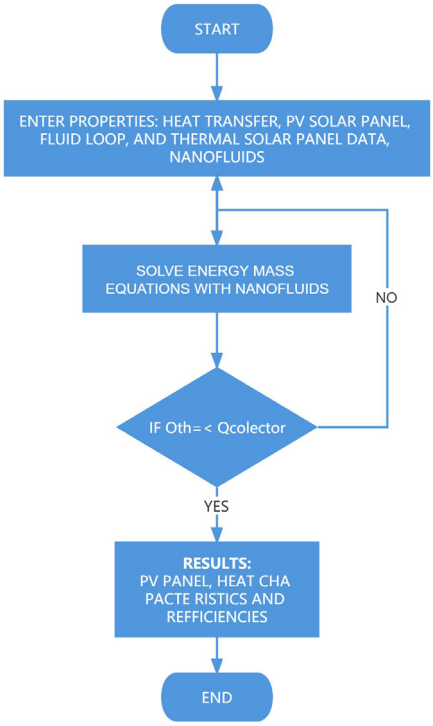

Figure 3. Logical flow diagram for finite difference scheme[20].

3 DISCUSSION AND ANALYSIS

Equations (1) through (17) have been coded in finite-difference forms, integrated, and numerically solved as per the logical diagram in Figure 3. In the following sections, we also present the analysis and discussions of these numerical results as well as the validations of the proposed simulation model using experimental data published in the literature. Samples of the predicted results for various nanoparticles; Al_2O_3, CuO, Fe_3O_4, and SiO_2 that drive the thermoelectric unit are presented. It is worthwhile noting that the numerical simulation presented was performed under different conditions such as; PV cell temperatures from 10°C through 70°C, ambient temperatures from 10°C

through 38°C, and solar radiations; 550, 750, 1000, and 1200w/m^2.

For numerical simulation of the model, the PV solar collector's specifications were obtained from Fargali et al[33]. The characteristic curves of the PV solar panel were also obtained from the manufacturer's specification sheet[33]. Interested readers in the full disclosure of the PV parameters are advised to consult Fargali et al.[33] and Sami and Marin[20].

The values of seebeck coefficient (SM), electrical resistance (RM), and thermal conductance (KM) are given in equations (10) through (21) and were selected over a range of -100°C to +150°C, according to the industry-standard thermoelectric, interested readers in the specifications of this module are advised to consult articles[11,13,20]. It should also be noted that the ambient temperature is considered 25°C for thermoelectric calculations. The TEG device was attached tightly to the heat sink, to ensure and maximize the heat dissipation at the bottom of the module.

The predicted results of the nanofluids were simulated at flows vary from 0.00697kg/s to 0.0345kg/s, nanoparticles volumetric concentrations from 0.01 to 0.5 and under solar radiations from 550W/m^2 to 1200W/m^2. The thermal tubes welded to the back of the PV solar panel were designed at a mass flow rate of 0.00697kg/s at 550W/m^2 solar radiation. Some studies[20,25,31] have demonstrated clearly that increasing the PV cell temperature increases the back-cell temperature, the heat transport fluid temperature, and the higher the solar radiation the higher the PV cell temperature.

Current-voltage curves and other characteristics of the TEG hybrid under different solar radiation and nanofluids HTF using Al_2O_3. The results showed that the higher the solar radiation the higher better the characteristics of the TEG. Figure 4 through Figure 7 under solar radiation 750w/m^2 and different nanofluid Al_2O_3 concentrations, showed that the nanofluid concentration significantly contributed to the enhancement of the key critical parameters of the TEG-PV-Thermal hybrid system in question. Thus, the simulated results showed the impact of the nanofluid Al_2O_3 on the power output of the TEG device, where the higher the nanofluid concentrations the higher the output current, and voltage as well as power over that of the water as base HTF. It is quite evident that 50%, Al_2O_3 nanofluid concentration produces the higher power output characteristics, however, it is extremely important to examine and take into account the pressure drop and other side effects associated with higher concentrations on the flow conditions and system efficiency. Also, the results demonstrated the benefits of using nanofluids in enhancing the thermal heat recovered from the PV-Th collectors that drive the TEG device and also the thermal heat dissipated from the TEG as presented in Figure 8.

In our opinion, higher nanoparticle concentrations increase the thermal, thermophysical, and heat transfer properties of the nanofluid such as specific heat, density, thermal conductivity, and viscosity as well as the convection heat transfer coefficient. This in turn enhances the thermal heat absorbed by the nanofluid. The impact of nanofluids other than Al_2O_3 on the critical parameters of the PV-Thermal and TEG device will be discussed elsewhere in the paper. On the other hand, Figure 8 and Figure 9 showed that the higher the concentration of the nanofluid Al_2O_3 the higher the heat transfer to heat transport nanofluid and the higher the thermoelectric efficiency. The previously presented was applied to interpret these findings.

The TEG device and the hybrid system efficiencies are presented in Figures 9 and 10, respectively. The results in these figures showed that the higher the Al_2O_3 nanofluid's concentration enhances the efficiency of the thermoelectric device and the hybrid system over that of the water as base HTF. In general, the results displayed in these figures clearly show that the higher the solar radiation the higher the thermal heat released from the PV-Th solar panel to the HTF, the higher the power produced by the thermoelectric device, and also the higher the efficiencies. The effect of nanofluids other than Al_2O_3 on the efficiencies of TEG devices and the hybrid system will be discussed elsewhere in the paper.

In particular Figure 11 showed the thermoelectric efficiency at different solar radiations using nanofluid Al_2O_3. These results indicated that higher solar radiations enhanced the thermal heat transfer to the thermoelectric device and its power produced as well as its efficiency.

On the other hand, Figures 12 to 15 displayed the impact of using the different nanofluids suspended particles of the Al_2O_3, CuO, Fe_3O_4, and SiO_2, on the TEG characteristics including efficiencies of the thermoelectric and hybrid system, respectively. In these figures, the nanofluid concentration varies between 0.01 to 0.50 with solar radiation of 750W/m^2 with the different parameters numerically calculated at 1000 seconds. Also, the results in these figures show a higher concentration of nanofluid enhances the characteristics of the TEG over water as a basic fluid. In our opinion, these observations can explain that higher nanoparticle concentrations enhance heat transfer properties of the HTF such as specific heat, density, thermal conductivity, and viscosity as well as the convection heat transfer coefficient. That increases stimulated and droved more heat transfer from the PV-Th solar panel into the nanofluid. This in turn also drove more heat into the TEG device and generates more power and enhances its efficiencies. It is also worthwhile noting that the PV solar

https://www.doi.org/10.53964/jmge.2022005

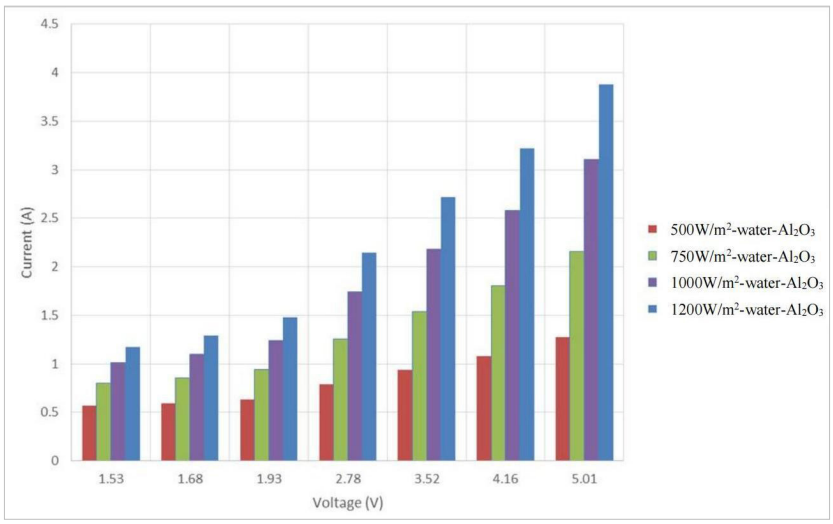

Figure 4. TEG characteristics using waster at different solar radiations.

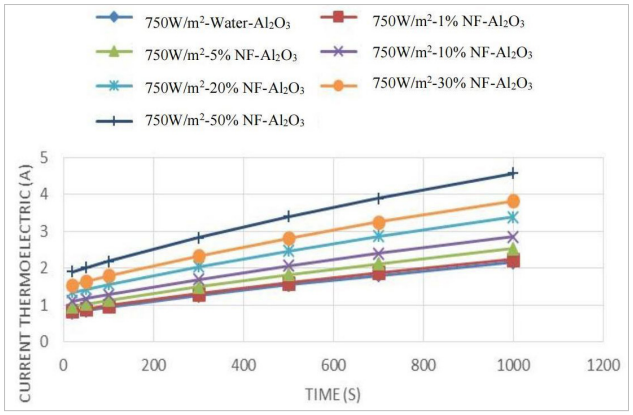

Figure 5. Thermoelectric current at different time steps and concentrations of Nanofluid Al_2O_3 at 750W/m^2.

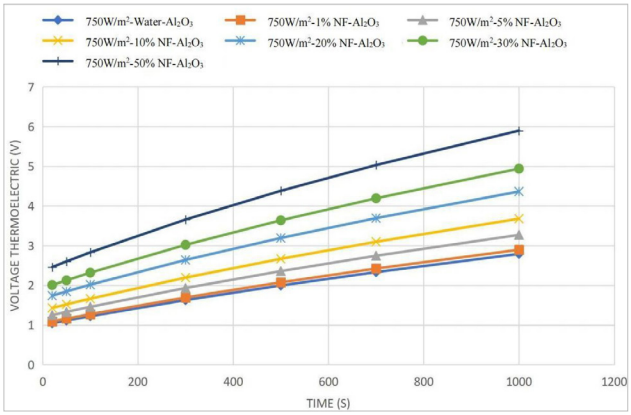

Figure 6. Thermoelectric voltage at different times and concentrations of nanofluid Al_2O_3 at 750W/m$_2$.

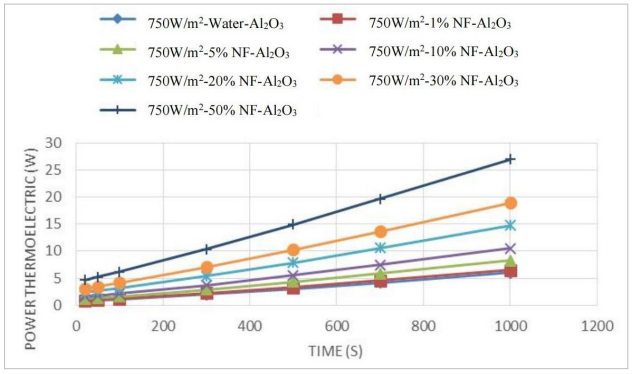

Figure 7. Thermoelectric power at different time steps and concentrations of Nanofluid Al_2O_3 at 750W/m^2.

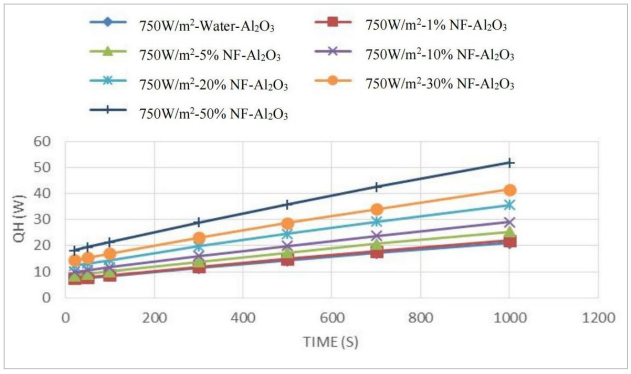

Figure 8. Thermoelectric heat released to ambient at different concentrations of nanofluid Al_2O_3 at 750W/m^2.

panel output power and PV solar panel efficiency remain constant and are fully not dependent on the nanofluids concentrations.

Furthermore, the results displayed in the aforementioned figures indicated that the TEG device characteristics were significantly higher with the use of nanofluid Fe_3O_4 and they increase as the concentration of these nanofluid particles increases over the water as basic heat transfer flow. It is also believed that this is attributed to the higher thermophysical and thermodynamic as well as heat transfer properties of nanofluid Fe_3O_4 compared to the other nanofluids under investigation. And demonstrated that at higher solar radiation, the nanofluid Fe_3O_4 enhanced the TEG and hybrid system efficiencies over the base fluid water. Furthermore, at a low nanofluid concentration of 1%, there

https://www.doi.org/10.53964/jmge.2022005

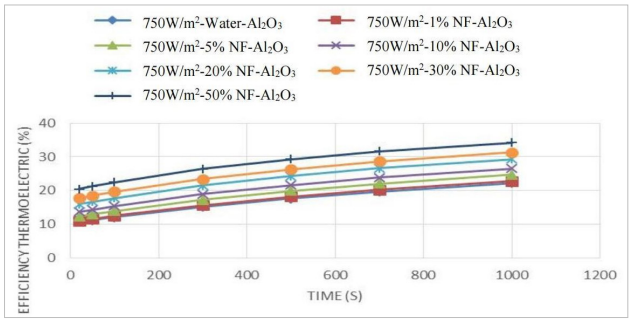

Figure 9. Thermoelectric efficiency at different concentrations of nanofluid Al_2O_3.

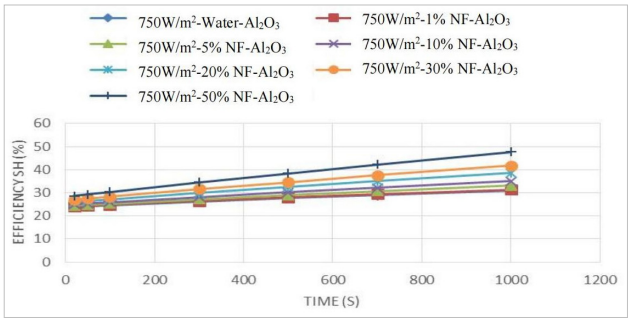

Figure 10. Efficiency of hybrid; solar PV-Th and thermoelectric at different concentrations of Nanofluid Al_2O_3 at 750W/m^2.

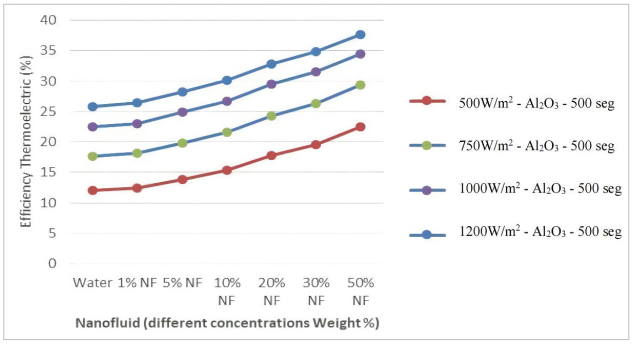

Figure 11. Thermoelectric efficiency at different solar radiations.

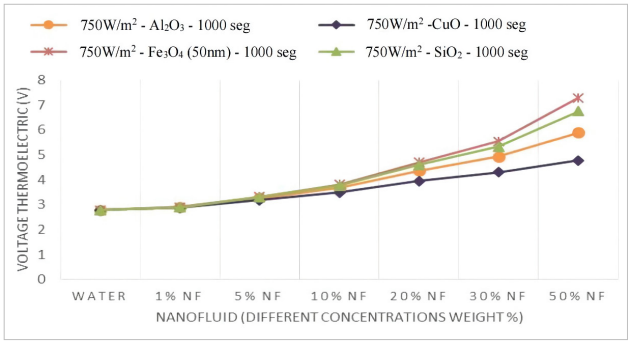

Figure 12. Thermoelectric voltage at different nanofluids.

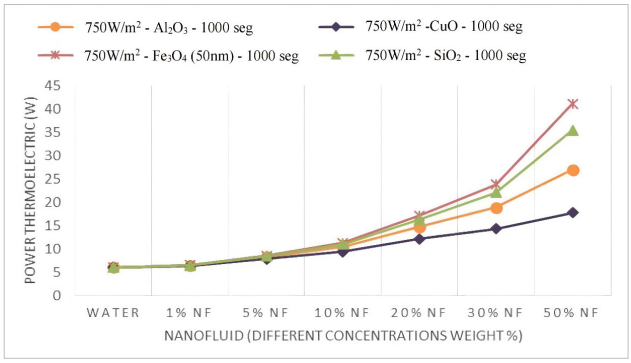

Figure 13. Thermoelectric output power at different nanofluids.

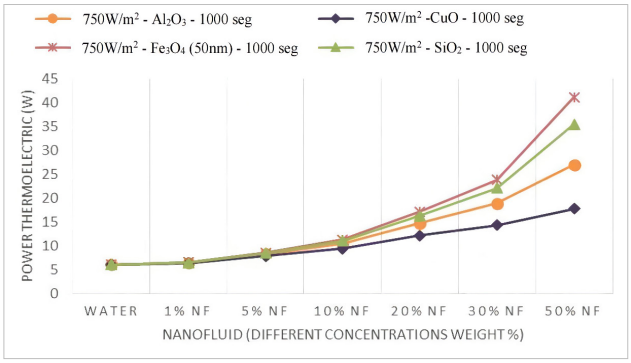

Figure 14. Thermoelectric efficiency at different nanofluids.

is no noticeable difference in the impact of the nanoparticles of the Al_2O_3, Fe_3O_4, CuO, and SiO_2. Furthermore, other studies were reported in the literature by Maiga et al.[41], and some researchers[32,35-45] confirmed our findings that the inclusion of nanoparticles into the base fluids has produced a considerable augmentation of the heat transfer coefficient, thermal heat transferred and TEG efficiencies.

3.1 Model Validation

This section is intended to validate the model prediction of the different parameters of the PV-Th and TEG device presented in equations (1) through (17) with different experimental data reported in the open literature on nanofluids and base fluids.

Figure 16 displays a comparison between the model prediction of the temperature and the data of Fargali et al[33]. The data showed that the model fairly compares with the data reported by Fargali et al[33]. This figure showed that the model and data have some discrepancies exist. It is believed that the discrepancies are because the various parameters used in equations (6) through (9) were not fully disclosed by Fargali et al[33]. However, the same observations were reported in the published articles[24-26].

TEG experimental data is scared in the literature. Recently Data published by Al Musleh et al.[45] on the TEG with a very low-low temperature difference between the hot and cold sides were selected for validating our model. The

https://www.doi.org/10.53964/jmge.2022005

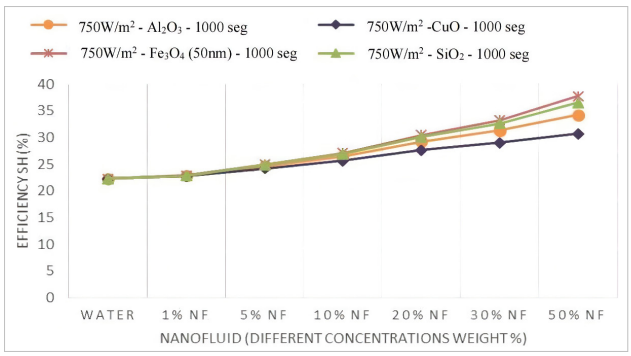

Figure 15. Hybrid system efficiency at different nanofluids.

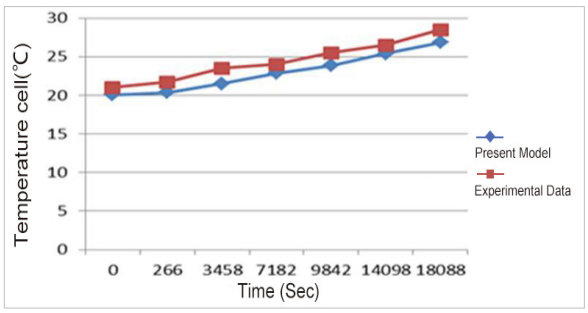

Figure 16. Comparison between model prediction and experimental data[31].

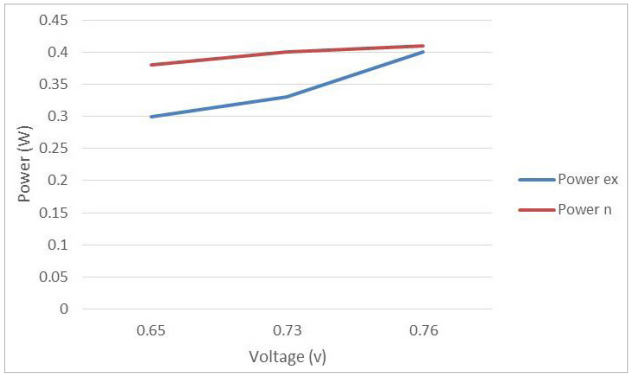

Figure 17. Comparison between the model prediction of TEG power and experimental data[45].

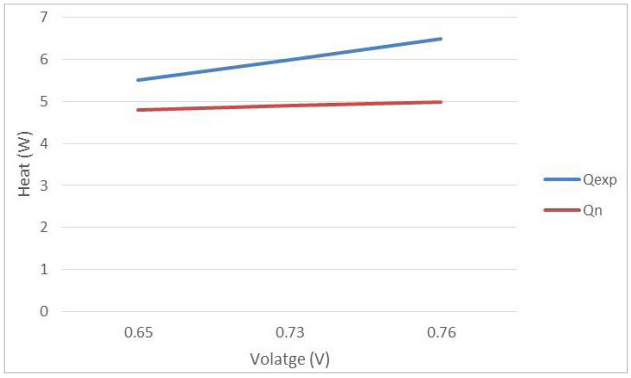

Figure 18. Comparison between the model prediction of TEG heat and experimental data[45].

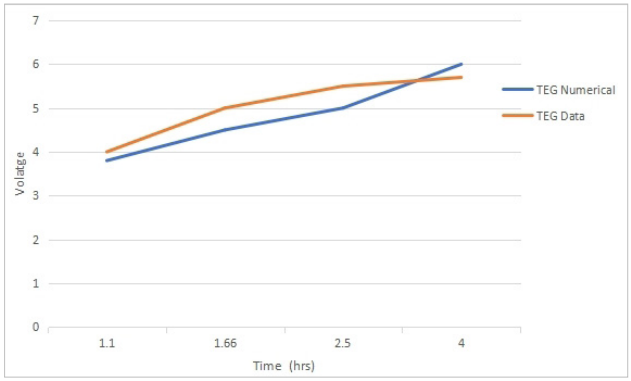

Figure 19. Comparison between TEG numerical and TEG data[40].

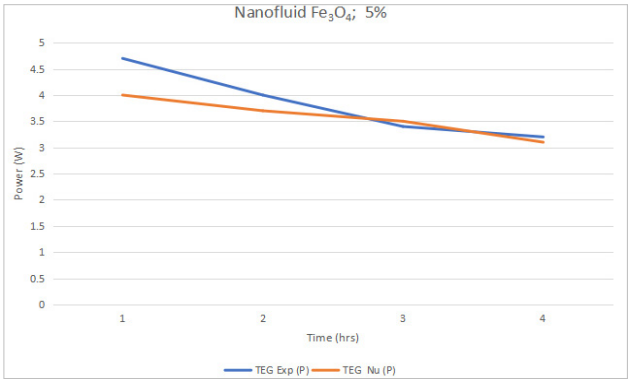

Figure 20. Comparison between TEG numerical and TEG data[4] at 5% Fe_3O_4.

experimental results reported in Al Musleh et al.[45] used a TEG experimental test setup with a temperature-controlled hotplate to provide accurate TEG performance. Data at the very-low-temperature difference were simulated and compared to our model numerical prediction and presented in Figure 17.

The temperatures of the driving heat source (hotplate) to the TEG were matched with the temperatures of the heat transport fluid heated by thermal energy dissipated from the PV-Th solar panel due to solar radiation. In general, as shown in Figure 18, our model's prediction compared fairly with the data reported by Al Musleh et al.[45] of voltage across the TEG. Furthermore, Figure 18 demonstrated that our model also fairly predicted the TEG power data of Al Musleh et al[45]. There are discrepancies observed, where our model underpredicted the power and over-predicted the heat experimental data. In our opinion, the discrepancies between our model's prediction and the data of Al Musleh et al.[45] are attributed to the fact our model does not take into consideration the heat losses from the TEG during the energy conversion process and also due to the inaccuracy of the empirical relationships used to calculate the module's key parameters such as the effective SM, RM, and KM.

A solar-driven exhaust air thermoelectric heat pump recovery system thermoelectric heat pump was tested and evaluated by Liu et al.[40] for its ability to recover

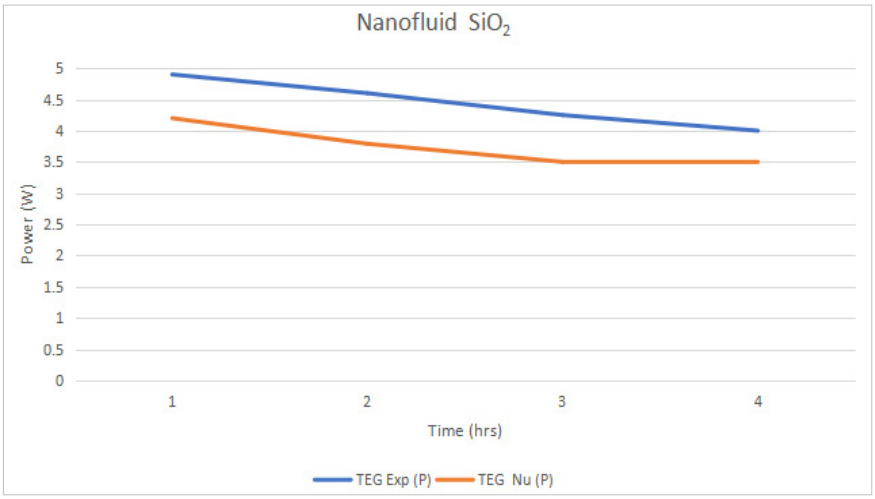

Figure 21. Comparison between TEG numerical and TEG data[47] at 5% SiO_2.

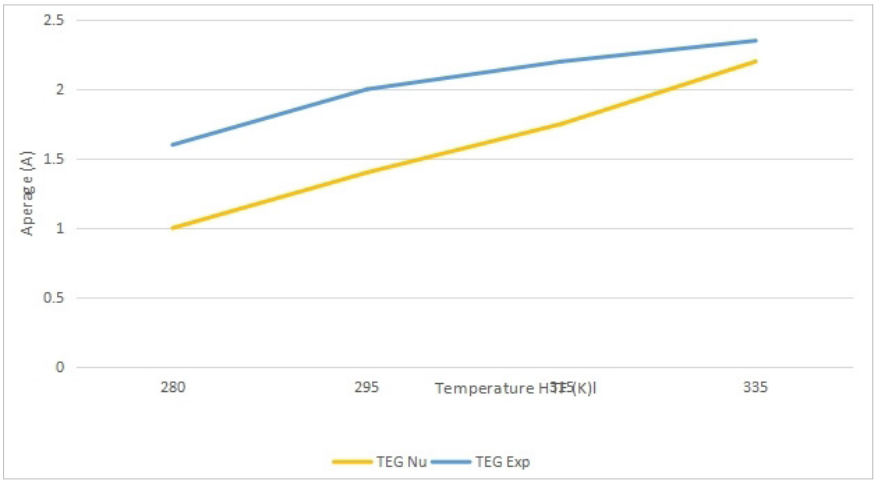

Figure 22. Comparison between TEG numerical prediction and TEG data[48].

thermal energy from exhaust air to cool or heat fresh air. An experimental platform was established to test its performance. The system required only 3.12W of power for the fans, which are powered by Thermoelectric units. The experimental data collected during this study was simulated and compared to our model prediction in Figure 19. It's quite from the comparison in this figure that the model predictions fairly predicted the TEG data of Liu et al[40].

A new nanofluid-based cooling method for a hybrid PV/thermoelectric system experimental data has been reported by Soltani et al.[47] and compared with our model prediction and presented in Figures 20 and 21 for Fe_3O_4 and SiO_2 respectively, at concentration 5%. The data reported in the article from Soltani et al.[47] were investigated experimentally, namely, natural cooling, forced air cooling, water cooling, SiO_2/water nanofluid cooling, and Fe_3O_4/water nanofluid cooling. In Figures 20 and 21 our model predictions were compared only to the cooling data of the two nanofluids Fe_3O_4 and SiO_2.

It is quite apparent from the comparison presented in the two Figures 20 and 22 that our model fairly predicted the data of the two nanofluids reported in the article from Soltani et al.[47], however, some discrepancies exited at the early time intervals and were less at higher time intervals. However, our predictions had fewer discrepancies with the nanofluid Fe_3O_4. That led us to believe that our correlations in Table 1 are more accurate for calculating the thermophysical properties for Fe_3O_4 than SiO_2.

Demir[48] proposed in his Ph.D. thesis a trigeneration system for electricity, hydrogen, and clean water production. TiO_2 photocatalyst using a photoelectrochemical (PEC) reactor, which cleans the water via a Fenton-like process and produces hydrogen. A novel solar TEG unit drives the reactor. And a phase change material which was heated by the concentrator feeds TEG, and the wastewater stream provides the cold surface. The PEC system was investigated experimentally and numerically. Figure 22 presented a comparison of the data from Demir[48] and our model's prediction of the amperage of the TEG at different HTF temperatures. The comparison in this figure showed the discrepancy between our model and the data of Demir[48]. It appeared that the discrepancy was bigger at a lower temperature than compared to higher temperatures. This

can be interpreted that the Peltier, Seebeck, and Thomson effects were more developed and accurate at higher temperatures of the heat transport fluid than at lower ones, thus the discrepancies were minimized and the model's prediction improved at higher temperatures.

4 CONCLUSION

During this study, the behavior of PV-Thermal and TEG were presented. In addition, the characteristics of nanofluids Al_2O_3, CuO, Fe_3O_4, and SiO_2 circulating in PV-Thermal solar panels and driving the TEG were also presented. Furthermore, key parameters of the TEG have been modeled and integrated into the present model. Finally, the results were discussed and compared to experimental data.

The model in this study was established after the mass and energy conservation equations coupled with the heat transfer equations nanofluids; Al_2O_3, CuO, Fe_3O_4, and SiO_2, and the key parameters of the TEG. The concentrations of the nanoparticles vary from 1% to 50%. Thermodynamic, thermophysical, and heat transfer properties of the nanofluids were obtained from the available data in the literature. The results presented hereby showed that the higher the nanoparticles concentration increase the thermal heat released by the PV-Th panel, and the higher the power generated by the thermoelectric device. Furthermore, it was also shown that higher nanoparticle concentration increased the heat transfer properties of heat transferred to the nanofluid, this increased the TEG device efficiency and the hybrid system efficiency. In addition, numerical results also showed that the nanofluid Fe_3O_4 has the highest thermal heat transfer to HTF and the highest TEG and hybrid efficiencies.

Finally, the numerical model predicted results fairly compared with the data reported in the literature on PV solar panels and TEG.

Acknowledgements

The research work presented in this paper was made possible through the support of TransPacific Energy, Inc.

Conflicts of Interest

The author declared no conflict of interest.

Author Contribution

Howard SS contributed to the manuscript and approved the final version.

Abbreviation List

HTF, Heat transfer fluid
KM, Thermal conductance
PEC, Photoelectrochemical
PV, Photovoltaic
RM, Electrical resistance
SM, Seebeck coefficient
TEG, Thermoelectric generators

References

[1] Richner P, Gaspar PD, Gonçalves LCC et al. The experimental results analysis of the energy conversion efficiency of thermoelectric generators. *RE&PQJ*, 2011; 1: 278-282. DOI: 10.24084/repqj09.312

[2] The Science of Thermoelectric Materials. The Seebeck Effect. Thermoelectric Caltech Materials Science, Thermoelectrics. Retrieved on January 3, 2013. Available at http://www.its.caltech.edu/~jsnyder/thermoelectrics/#top

[3] Snyder G, Toberer E. Complex thermoelectric materials. *Nature Mater*, 2008; 7: 105-114. DOI: 10.1038/nmat2090

[4] Rowe DM ed. CRC Handbook of Thermoelectrics. CRC Press: Florida, USA, 1995; 7-9.

[5] Snyder GJ, Ursell TS. Thermoelectric efficiency and compatibility. *Phys Rev Lett*, 2003; 91: 148301. DOI: 10.1103/PhysRevLett.91.148301

[6] Thermal Radiation: Planck's Law. Warren M. Rohsenow Heat And Mass Transfer Laboratory. Accessed on January 3, 2013. Available at: http://ocw.mit.edu/courses/mechanical-engineering/2-997-direct-solar-thermal-to-electricalenergy-conversion-technologies-fall-2009/audio-lectures/MIT2_997F09_lec02.pdf

[7] Custom Thermoelectric. History of Thermoelectrics. Accessed January 3, 2013. Available at http://www.customthermoelectric.com/History.html

[8] DiSalvo FJ. Thermoelectric cooling and power generation. *Science*, 1999; 285: 703-706. DOI: 10.1126/science.285.5428.703

[9] Rowe DM. Thermoelectrics, an environmentally-friendly source of electrical power. *Renew Energ*, 1999; 16: 1251-1256. DOI: 10.1016/S0960-1481(98)00512-6

[10] Yildiz F, Coogler KL, Crockford B. An applied compares study: Solar energy vs. thermoelectric energy: 120th ASEE Annual & Exposition, Atlanta, US, 23-26 June 2013.

[11] US. Ferrotec USA. Ferrotec's Thermoelectric Technical Reference Guide is a comprehensive technical explanation of thermoelectrics and thermoelectric technology. Accessed 2022. Available at https://thermal.ferrotec.com/technology/thermoelectric-reference-guide/2014

[12] Dziurdzia P, Tan YK. Modeling and simulation of thermoelectric energy harvesting processes. In: Sustainable Energy Harvesting Technologies-Past, Present and Future, 2011; 109-116.

[13] Patel J, Patel M, Patel J et al. Improvement in the COP of thermoelectric cooler. *Int J Sci Tech Res*, 2016; 5: 73-76.

[14] Beeby S, White N. Energy Harvesting for Autonomous Systems. Artech House: Nowood, MA, 2010.

[15] Buist RJ. Calculation of Peltier device performance, CRC Handbook of Thermoelectrics. CRC Press: Florida, USA, 1995; 143-155.

[16] Chen M, Rosendahl LA, Condra TJ et al. Numerical modeling of thermoelectric generators with varing material properties in a circuit simulator. *IEEE T Energy Conver*, 2009; 24: 112-124. DOI: 10.1109/TEC.2008.2005310

[17] Dalola S, Ferrari M, Ferrari V et al. Characterization of thermoelectric modules for powering autonomous sensors.

IEEE T Instrum Meas, 2008; 58: 99-107. DOI: 10.1109/TIM.2008.928405

[18] De Baetselier E, De Mey G, Kos A. Thermal image generator as a vision prosthesis for the blind. *MST Poland News*, 1997; 3: 7.

[19] De Baetselier E, Goedertier W, De Mey G. Thermoregulation of ICs with high power dissipation: Proceedings of the 10th European hybrid Microelectronics Conference, Copenhagen, Denmark, May 1995.

[20] Sami S, Marin E. Modelling and simulation of PV solar-thermoelectric generators using nano fluids. *Int J Sustain Energy*, 2019; 8: 70-99. DOI: 10.18488/journal.13.2019.81.70.99

[21] Dziurdzia P, Kos A. Electrothermal macromodel of active heat sink for cooling process simulation: International workshop on thermal investigations of ICs and microstructures, Rome, 03-06 October 1999.

[22] Dziurdzia P, Kos A. High-Efficiency Active Cooling System: Proceeding of the XVIth Annual IEEE Semiconductor Thermal Measurement and Management Symposium, San Jose, USA, 21-23 March 2000. DOI: 10.1109/STHERM.2000.837057

[23] Freunek M, Müller M, Ungan T et al. New physical model for thermoelectric generators. *J Electron Mater*, 2009; 38: 1214-1220. DOI: 10.1007/s11664-009-0665-y

[24] Hashim H, Bomphrey JJ, Min G. Model for geometry optimisation of thermoelectric devices in a hybrid PV/TE system. *Renew Energy*, 2016; 87: 458-463. DOI: 10.1016/j.renene.2015.10.029

[25] Liang R, Zhang J, Zhou C. Dynamic simulation of a novel solar heating system based on hybrid photovoltaic/thermal collectors (PVT). *Procedia Eng*, 2015; 121: 675-683. DOI: 10.1016/j.proeng.2015.09.001

[26] Sami S, Campoverde C. Dynamic simulation and modeling of a novel combined hybrid photovoltaic-thermal panel hybrid system. *Int J Sustain Energy Environ Res*, 2018; 7: 1-23. DOI: 10.18488/journal.13.2017.71.1.23

[27] Sami S. Modeling and simulation of a novel combined solar Photovoltaic-Thermal panel and heat pump hybrid system. *Clean Technol-Basel*, 2018; 1: 89-113. DOI: 10.3390/cleantechnol1010007

[28] Sami S, Marin E. Simulation of solar photovoltaic, biomass gas turbine and district heating hybrid system. *Int J Sustain Energy Environ Res*, 2017; 6: 9-26. DOI: 10.18488/journal.13.2017.61.9.26

[29] Sami S, Rivera J. A predictive numerical model for analyzing performance of solar photovoltaic, geothermal hybrid system for electricity generation and district heating. *Sci J Energ Eng*, 2017; 5: 13-30. DOI: 10.11648/j.sjee.20170501.12

[30] Sami S, Marin E. A numerical model for predicting performance of solar photovoltaic, biomass and CHP hybrid system for electricity generation. *Int J Eng Sci Res Technol*, 2017; 4: 1-22.

[31] Good C, Chen J, Dai Y et al. Hybrid photovoltaic-thermal systems in buildings-a review. *Energ Procedia*, 2015; 70: 683-690. DOI: 10.1016/j.egypro.2015.02.176

[32] Sagadevan S. A review on role of nanofluids for solar energy applications. *Am J Nano Res Appl*, 2015; 3: 53-61. DOI: 10.11648/j.nano.20150303.14

[33] Fargali HM, Fahmy FH, Hassan MA. A simulation model for predicting the performance of PV/wind-powered geothermal space heating system in Egypt. *Online J Electron Electr Eng*, 2008; 2: 321-330.

[34] Gang P, Huide F, Tao Z et al. A numerical and experimental study on a heat pipe PV/T system. *Sol Energy*, 2011; 85: 911-921. DOI: 10.1016/j.solener.2011.02.006

[35] Chaudhari KS, Walke PV. Applications of nanofluid in solar energy-a review. *Int J Eng Res*, 2014; 3: 460-463.

[36] Kasaeian A, Eshghi AT, Sameti M. A review on the applications of nanofluids in solar energy systems. *Renew Sust Energ Rev*, 2015; 43: 584-598. DOI: 10.1016/j.rser.2014.11.020

[37] Ramos-Castañeda CF, Olivares-Robles MA, Méndez-Méndez JV. Analysis of the performance of a solar thermoelectric generator for variable leg geometry with nanofluid cooling. *Processes*, 2021; 9: 1352. DOI: 10.3390/pr9081352

[38] Sani E, Martina MR, Salez TJ et al. Multifunctional magnetic nanocolloids for hybrid solar-thermoelectric energy harvesting. *Nanomaterials*, 2021; 11: 1031. DOI: 10.3390/nano11041031

[39] Sami S. Enhancement of performance of thermal solar collectors using nanofluids. *Int J Energy Power Eng*, 2018; 7: 1-8. DOI: 10.11648/J.IJEPE.S.2018070101.11

[40] Liu Z, Li W, Zhang L et al. Experimental study and performance analysis of solar-driven exhaust air thermoelectric heat pump recovery system. *Energ Buildings*, 2019; 186: 46-55. DOI: 10.1016/j.enbuild.2019.01.017

[41] Maiga SEB, Palm SJ, Nguyen CT et al. Heat transfer enhancement by using nanofluids in forced convection flows. *Int J Heat Fluid Fl*, 2005; 26: 530-546. DOI: 10.1016/B978-0-7506-9185-7.50017-9

[42] Khullar V, Tyagi H, Phelan PE et al. Solar energy harvesting using nanofluids-based concentrating solar collector. *J Nanotechnol Eng Med*, 2012; 3: 031003. DOI: 10.1115/1.4007387

[43] Azo Material, 2004. Accessed 2022. Available at http://www.azom.com/properties.aspx

[44] Brenner H, Edwards DA, Wasan DT. Interfacial Transport Process and Rheology. Butterworth: New York, USA, 1993.

[45] Al Musleh M, Topriska E, Jack L et al. Thermoelectric generator experimental performance testing for wireless sensor network application in smart buildings: MATEC Web of Conferences. *EDP Sciences*; 2017. DOI: 10.1051/matecconf/201712008003

[46] Biswas O, Kandasamy P. Development and experimental investigation of portable solar-powered thermoelectric cooler for preservation of perishable foods. *Int J Renew Energy R*, 2021; 11: 1292-1303.

[47] Soltani S, Kasaeian A, Sarrafha H et al. An experimental investigation of a hybrid photovoltaic/thermoelectric system with nanofluid application. *Sol Energy*, 2017; 155: 1033-1043. DOI: 10.1016/j.solener.2017.06.069

[48] Demir ME. Experimental investigation of an integrated solar driven wastewater treatment system for trigeneration applications [doctor's thesis]. Ontario, Canada: University of Ontario Institute of Technology; 2018.